

High resolution scanning tunneling spectroscopy of ultrathin Pb on Si(111)-(6 × 6) substrate

M. Krawiec, M. Jabchoński and M. Kisiel

Institute of Physics and Nanotechnology Center, M. Curie-Skłodowska University, pl. M. Curie Skłodowskiej 1, 20-031
Lublin, Poland

Abstract

The electronic structure of Si(111)-(6 × 6)Au surface covered with submonolayer amount of Pb is investigated using scanning tunneling spectroscopy. Already in small islands of Pb with thickness of 1 ML Pb₍₁₁₁₎ and with the diameter of only about 2 nm we detected the quantized electronic state with energy 0.55 eV below the Fermi level. Similarly, the I(V) characteristics made for the Si(111)-(6 × 6)Au surface reveal a localized energy state 0.3 eV below the Fermi level. These energies result from fitting of the theoretical curves to the experimental data. The calculations are based on tight binding Hubbard model. The theoretical calculations clearly show prominent modification of the I(V) curve due to variation of electronic and topographic properties of the STM tip apex.

Key words: Scanning tunneling spectroscopies, Surface electronic phenomena, Metallic quantum wells, Tunneling
PACS: 73.20.-r, 73.20.At, 73.40.Gk, 73.63.Kv, 73.63.Hs

1. Introduction

Spectacular observations of electron confinement in Pb quantum wells (QW) have been realized in several photoemission spectroscopy (UPS) experiments [1], [2], [3], helium atom scattering [4], [5], and in in situ electrical resistivity measurements [6]. These techniques only provide surface electronic structure information averaged over a large surface area. In contrast, the scanning tunneling microscopy (STM), and scanning

tunneling spectroscopy (STS) allow one to study topographic and electronic structure with atomic scale resolution [7], [8], and [9]. STS was also successfully applied for studying the quantum size effects (QSE) in well defined Pb islands, starting with the smallest thickness of 3 monoatomic layers (ML) [10] and laterally rather large. In our previous UPS study we have shown that even 1 ML thick layer of Pb shows distinct QSE discrete electronic level. However, clear experimental evidence directly relating quantized electronic states with lateral size of individual islands has not been reported. In the initial stage of ultrathin film growth, for very low coverage, effects associated with formation of quantum dots are expected and the STS technique is particularly well suited to

Corresponding author, tel.: +48 81 537 6285, fax: +48 81 537 6191

Email addresses: krawiec@kft.umcs.lublin.pl (M. Krawiec), ifmkj@tytan.umcs.lublin.pl (M. Jabchoński), mkisiel@tytan.umcs.lublin.pl (M. Kisiel).

detect and to study these phenomena. However, quantitative analysis of tunneling current versus sample bias $I(V)$ dependence requires knowledge of the tunneling tip shape and its electronic structure. Both parameters are in general unknown.

In this paper, we investigate the topographic and electronic structure of small Pb islands and single Pb atoms on Si(111)-(6 \times 6)Au surface by means of low temperature atomically resolved scanning tunneling spectroscopy. The experimental studies are supplemented by theoretical ones based on a tight binding model, where the $I(V)$ characteristics are calculated using the non-equilibrium Keldysh Green function formalism. We demonstrate how (unavoidable during STS experiment) modification of the tunneling tip apex by uncontrolled attaching or detaching of a single atom, modify the $I(V)$ curve. Moreover, we present existence of well defined QSE electronic level in 1 ML thick Pb island with diameter smaller than 1.5 nm.

2. Experimental method and results

The experiment was carried out in UHV chamber equipped with an Omicron variable temperature STM and RHEED. After preparation of Si(111)-(6 \times 6)Au surface under RHEED control at room temperature (for further details of sample preparation see [1]) the sample was transferred into a cooled STM stage where a submonolayer amount of Pb was evaporated. STM tips were produced by conventional electrochemical etching of tungsten wire, and were further conditioned in situ via prolonged scanning over a clean Si(111)-(7 \times 7) surface with sample bias set within the range from -5 to -10 V. Tunneling spectroscopy was performed simultaneously with topography measurements at every point of the surface that is imaged by STM, or every fifth point sampled during a scan. Typical STS data file contained 5000 $I(V)$ curves with 200 $I(V)$ points each. The presented below STS curves are averages of several individual curves collected within indicated areas. The number of these curves spanned from 16 for smallest area, to 68 in the case of the largest area. The area sizes were chosen in such a way that the

individual curves were very much the same shape, typically within 20 % of the tunneling current at any bias. This inaccuracy, due to averaging, was further reduced. We stress that we have avoided presenting of data from areas where shapes of neighboring $I(V)$ curves were scattered and noisy. We are aware that averaging procedure applied for sufficiently large number of curves (even if they differ strongly) supplies nice, smooth curve. The $I(V)$ characteristics were acquired with feedback loop inactive. During the measurements the temperature of the sample was about 130 K and the base pressure was less than $6 \cdot 10^{-11}$ mbar.

Figure 1 shows example of high resolution topographic data of the Si(111)-(6 \times 6)Au surface with deposited 0.2 ML of Pb. The image shows separate Pb islands with diameter ranging from about 1 nm to maximum of about 3 nm. At the sample bias equal to -1.5 V the height of the largest islands is close to 0.4 nm. This corresponds to the height of a continuous monolayer of Pb(111). The visible smallest species have the width and the height equal to 1 nm and 0.17 nm, respectively. The largest islands have flat tops whereas the smaller appear as rounded features. We believe that the smallest features are single Pb atoms, similarly as in the samples with coverage as low as 0.012 ML of Pb(111) [1], whereas the largest one possesses crystalline structure continuous monatomic layer of Pb(111) [1].

In comparison with the constant current imaging mode operation of the STM, the spectroscopic mode requires cleanness and extra stability of the tip. Although the STM tip was carefully conditioned and its quality was checked during a control scan over freshly prepared Si(111)-(7 \times 7) surface, we have seen frequently reversible or irreversible changes of the tip properties. Although these changes influenced only slightly the topographic images of the surface, they have modified strongly the shape of the $I(V)$ tunneling characteristics. This is shown in Fig. 2 and 3. In Fig. 2 the tunneling characteristics taken on Si(111)-(6 \times 6)Au surface exhibit negative differential resistance. We stress that this phenomenon is related to the tip properties. In other measurements, made with other tip, the region with negative differential conductivity appeared only as shoulder shown

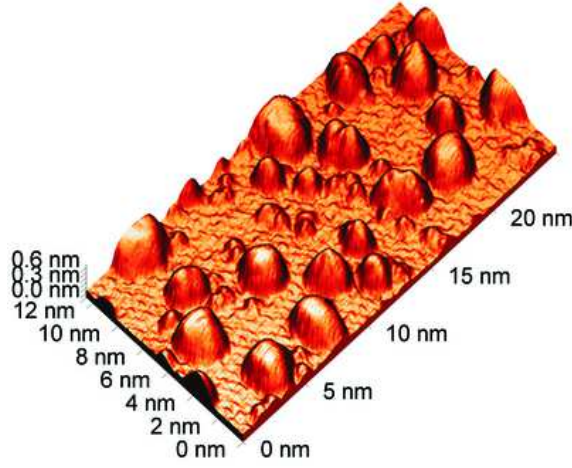


Fig. 1. STM image of Si(111)-(6x6)Au surface covered with 0.2 ML of Pb. The sample bias voltage was -1.5 V and the tunneling current was 0.5 nA. The largest islands have thickness equivalent continuous Pb(111) ML. The smallest species visible are single Pb atoms. Periodic modulation of the Si(111)-(6x6)Au reconstruction is also visible.

in Fig. 3. In general the negative differential conductivity was observed for the tips giving worse resolved topographic images.

3. Theoretical description

In general, the tunneling current depends on the Local Density of States (LDOS) of both tip and the sample [12], but in the most earlier experimental works no particular attention to the details of the LDOS of the tungsten tip has been paid. In order to explain the occurrence of the negative differential resistance and to correlate it with the tip shape, we have developed a model of the tunneling system with the tip which may attach a single atom or a cluster of atoms - a case which occurs frequently during scans.

The system composed of surface, island and STM tip, Fig. 4, is described by following Hamiltonian

$$H = H_{STM} + H_{tip} + H_{isl} + H_{surf} + H_{int}; \quad (1)$$

where

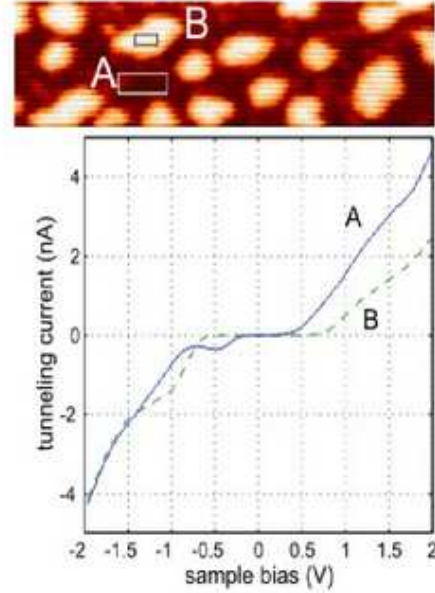


Fig. 2. 40nm x 10nm (400 x 100 pixels) STM image and I(V) characteristics of Si(111)-(6x6)Au surface covered with 0.2 ML of the Pb. The characteristics were acquired every fifth pixel. The curves A and B in the lower panel are averages over corresponding areas A and B shown in the upper panel of the Figure. The feedback loop was opened at 3.1 nA and -1.76 V.

$$H_{STM} = \sum_{k \in 2STM} \epsilon_k c_k^\dagger c_k \quad (2)$$

and

$$H_{surf} = \sum_{k \in 2surf} \epsilon_k c_k^\dagger c_k \quad (3)$$

stand for the STM and the surface electrodes electrons with the energies ϵ_k . The STM tip is modeled by a single atom with the energy level ϵ_0

$$H_{tip} = \epsilon_0 c_0^\dagger c_0; \quad (4)$$

Similarly the island is described by the energy level ϵ_i

$$H_{isl} = \epsilon_i c_i^\dagger c_i; \quad (5)$$

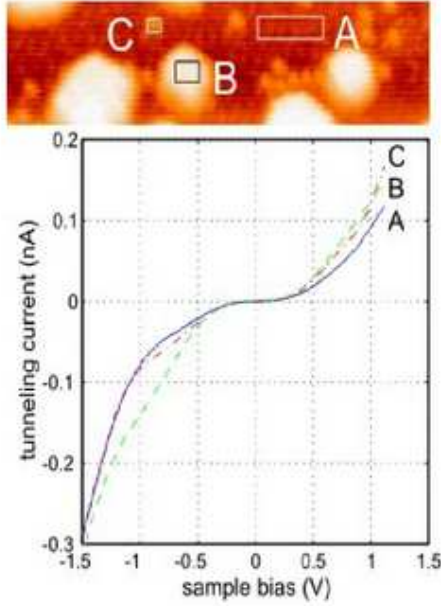


Fig. 3. 20nm x 5 nm (100 x 25 pixels) STM image and I(V) characteristics of Si(111)-(6 x 6)Au surface covered with 0.2 ML of Pb. The characteristics were acquired every pixel. The curves A, B, and C in the lower panel are averages over corresponding areas A, B, and C shown in the upper panel of the Figure. The feedback loop was opened at 0.5 nA and -1.76 V.

The interactions between different subsystems are in the form

$$H_{int} = \sum_{k \in \text{STM}} V_{k0} c_k^\dagger c_0 + t_{i0} c_0^\dagger c_i + \sum_{k \in \text{surf}} V_{ki} c_k^\dagger c_i + H_{sc} \quad (6)$$

with V_{k0} being a hybridization between the STM electrode and the STM tip, t_{i0} - the hopping integral between electrons on the island and those in the tip, and V_{ki} - hybridization connecting the surface and the island. Note that we have omitted the spin index in above equations as in this case spin channels can be treated separately.

In order to calculate the STM tunneling current

we follow the standard procedure [13] and the result reads

$$I = \frac{2e}{\hbar} \int_{-1}^1 \frac{dE}{2} T(E) [f_{STM}(E) - f_{surf}(E)]; \quad (7)$$

where $f_{STM(surf)}(E)$ is the Fermi distribution function and the transmittance $T(E)$ is given in the form

$$T(E) = \frac{\Gamma_{STM}(E) \Gamma_{surf}(E) |G_{i0}^r(E)|^2}{\Gamma_{STM}(E) \Gamma_{surf}(E) |G_{i0}^r(E)|^2 + \Gamma_{STM}(E) \Gamma_{surf}(E)} \quad (8)$$

$\Gamma_{STM}(E) = 2 \sum_{k \in \text{STM}} |V_{k0}|^2 \delta(E - \epsilon_k)$ and $\Gamma_{surf}(E) = 2 \sum_{k \in \text{surf}} |V_{ki}|^2 \delta(E - \epsilon_k)$ is the coupling parameter between STM electrode and the tip atom and surface and the island respectively. $G_{i0}^r(E)$ is the Fourier transform of the retarded Green's function $G_{i0}^r(t) = i \langle t \rangle \langle [c_i(t); c_0^\dagger(0)] \rangle$, connecting the tip atom 0 with the island.

In numerical calculations we have chosen a constant density of states in the STM electrode and the density of states in the surface $\rho_{surf}(E) = \delta(E - 0.06 \text{ eV})$. The parameter t_{i0} is equal to 2.5 eV, which corresponds to the tip-surface distance $z = 4 \text{ \AA}$ [14,15]. Such a small value of z stems from the fact that we have assumed the only single tunneling channel. In realistic situation there are many of them and if we take this effect into account the distance z will be larger.

To make comparison to the experiment and reproduce the STM data shown in Figs. 2 and 3, we have used two different model tips. The tip is described by a particle coupled to the STM electrode. Their coupling parameter Γ_{STM} depends on the tip sharpness and reflects a size of the particle attached to the tip electrode. The first one, which reproduces the results shown in Fig. 2, is characterized by a particle with energy level $\epsilon_0 = 0.8 \text{ eV}$ strongly coupled to the STM electrode $\Gamma_{STM} = 5 \text{ eV}$. This corresponds to the real STM tip with small curvature - blunt tip (BT), giving low resolution topographic images (see Fig. 2). The other one, reproducing the results shown in Fig. 3 and giving high resolution topographic images, is a sharp tip (ST) modeled by single atom with $\epsilon_0 = 2.0 \text{ eV}$ weakly coupled to the STM electrode $\Gamma_{STM} = 0.7 \text{ eV}$. Small value for the "sharp" tip describes localized,

atomic-like character of a single atom. Large coupling parameter represents a large cluster of atoms with bulk-like electronic structure. This is shown schematically in Fig.4.

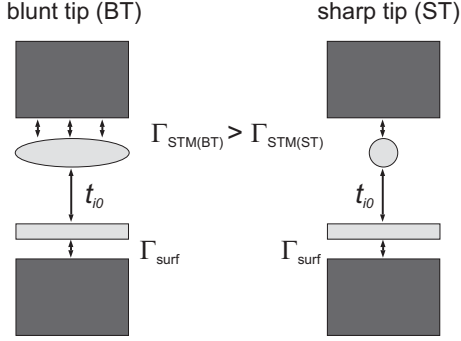


Fig. 4. Schematic representation of two tips considered in the tunneling current calculations. Larger coupling parameter Γ_{STM} represents a large cluster of atoms with bulk-like electronic structure. Smaller value of the coupling parameter reflects localized, atomic-like character of a single atom at the tip apex.

Figure 5 (a) shows the comparison of the experimental data of the STM current-voltage characteristic of the Pb island (curve B in Fig.2) and the theoretical calculations with a blunt tip. The theoretical calculation has been done with assumption that the Pb island is weakly coupled to the surface $\Gamma_{surf} = 0.6$ eV and a single particle state ϵ_i is at energy 0.55 eV with respect to the Fermi energy. We identify this single particle state energy with the quantum size state level in 1 ML of Pb, as it was determined in photoemission experiment [1]. The corresponding comparison for a sharp tip (curve B in Fig. 3) is shown in Fig. 5 (b). Note that the parameters characterizing the Pb island and the tip-surface distance are exactly the same as those previously used. Such huge modifications of the tunneling current are due to the properties of the tip only.

In order to reproduce the $I(V)$ characteristics of the Si(111)-(6x6)Au surface, we assumed that tunneling takes place into a small region of the surface, containing one or a few atoms, artificially isolated from the rest of the sample, which therefore can be also modeled as an island. This island is characterized by energy level $\epsilon_i = 0.3$ eV and the coupling to the rest of the surface Γ_{surf} is equal to 4 eV. The

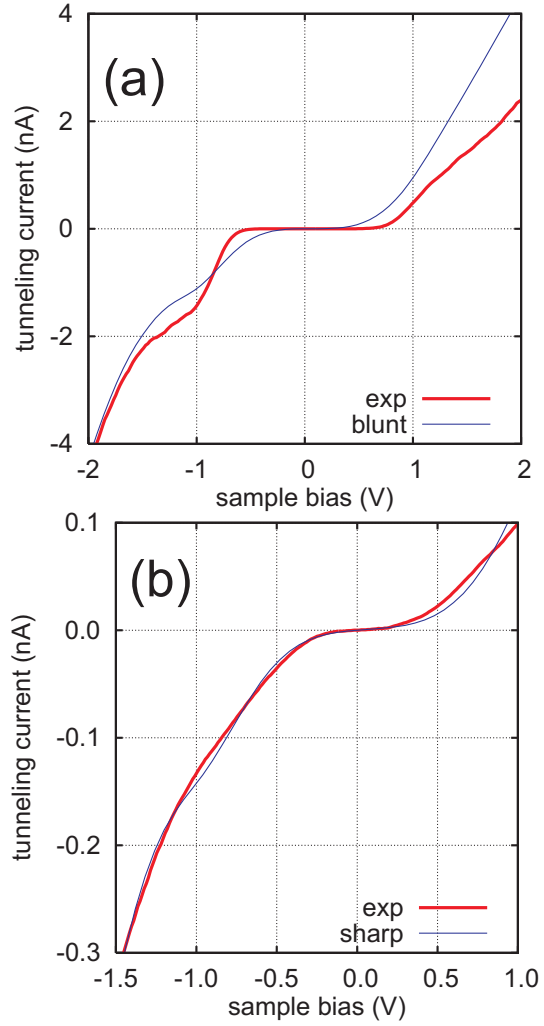


Fig. 5. The comparison of the $I(V)$ experimental data of the tunneling current to the Pb island (thick line) with theoretical calculation (thin line) for the blunt tip (a), and for the sharp tip (b), respectively. The model parameters are described in the text.

single particle energy level for Si(111)-(6x6)Au surface corresponds to energy of a δ state electron energy band found in photoemission experiment [16]. The other parameters are the same as previously used. The energies of the particles at the tip were chosen to fit the calculated curves to the experimental ones. The only consequence of their variation was change of the curves slope at higher biases but not the positions of the $I-V$ curves negative regions.

The comparison of the theoretical calculations

with the experimental data is shown in Fig. 6 (a). Note the negative behavior of the $I(V)$ character-

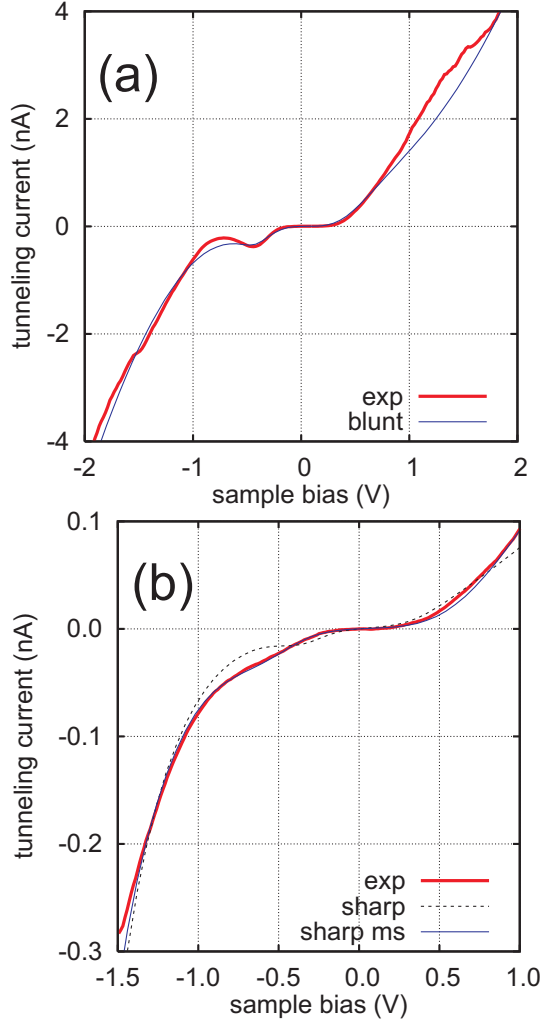


Fig. 6. The comparison of the $I(V)$ data of the tunneling current to the Si(111)-(6 \times 6)Au island (thick line) with theoretical t (thin line) for the blunt tip (a), and for the sharp tip (b), respectively. In (b) the dotted line corresponds to the coupling $\gamma_{\text{surf}} = 4$ eV and the solid one is for $\gamma_{\text{surf}} = 1$ eV. The other parameters are described in the text.

istic in a small region below sample bias $V = 0.5$ V. Corresponding results for the sharp tip are displayed in Fig. 6 (b).

If we use the same parameters characterizing the island as those in Fig. 5 (b) and sharp tip, we get quite reasonable agreement with the experimental

data (dotted line), except for small region around $V = 0.5$ V, which is the hallmark of the negative $I(V)$ characteristic observed in Fig. 6 (a). To im-

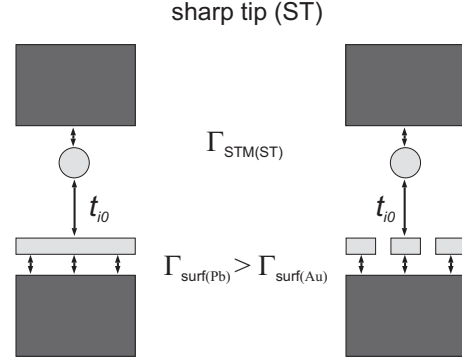


Fig. 7. Schematic representation of two surfaces modeled by islands. Larger coupling parameter $\gamma_{\text{surf}}(\text{Pb})$ represents Pb island. Smaller value of the coupling parameter $\gamma_{\text{surf}}(\text{Au})$ describes small area of surface embedded in the surrounding (6 \times 6)Au reconstruction and weakly coupled to the substrate.

prove this effect we had to make the coupling of the island to the surface smaller. A four times smaller γ_{surf} gives excellent agreement with the experimental results (thin solid line). We believe that the use of the smaller value of γ_{surf} has a physical origin and can be explained in the following way. For a sharp tip the tunneling takes place to a narrower region of the surface than in the case the blunt tip. This is well understood and accepted phenomenon. Therefore the surface region modeled by the isolated island is also smaller, containing less Au atoms (Fig. 7). Further, if we assume that each atom on the island is equally coupled to the surface we arrive at the conclusion that in this case the coupling γ_{surf} should be smaller. Only with this assumption we were able to get a perfect agreement with the experiment. Note that in the case of the Pb island no such modification of γ_{surf} is necessary, as the tunneling region is bounded by the Pb island itself. As one can read off from Fig. 1 the Pb islands are narrow and, more importantly, quite high (a few of Å), thus the tunneling directly into the surface can be neglected.

4. Conclusions

In conclusion we have performed STS studies of ultrathin Pb on Si(111)-(6 \times 6)Au surface supplemented by theoretical calculations based on tight binding model. Already in small islands of Pb with thickness of 1 ML Pb₍₁₁₁₎ and with the diameter of only about 2 nm the quantized electronic state with energy 0.55 eV below the Fermi level is detected. We identify this energy with the quantum well state of 1 ML thick Pb island seen in the UPS experiment [1]. Similarly, the I(V) characteristics made for the Si(111)-(6 \times 6)Au surface reveal localized energy state 0.3 eV below the Fermi level, previously detected in photoemission [16]. The obtained results lead also to the important conclusion that measured I(V) characteristics should be taken with care, as they strongly depend on the shape and the properties of the tip itself, which is often omitted while discussing and interpreting experimental data.

Acknowledgements

This work has been supported by grant no. 1 P 03B 004 28 of the Polish Committee of Scientific Research.

References

- [1] M. Jalochocki, H. Knoppe, G. Lilienkamp, and E. Bauer, Phys. Rev. B 46 (1992) 4693.
- [2] A. Mans, J. H. Dil, A. R. H. F. Ettema, and H. W eitering, Phys. Rev. B 66 (2002) 195410.
- [3] J. H. Dil, J. W. Kim, S. Gokhale, M. Tallarida, and K. Hom, Phys. Rev. B 70 (2004) 045405.
- [4] J. Braun and J. P. Toennies, Surf. Sci. 384 (1997) L858.
- [5] A. Crottini, D. Cvetko, L. Floreano, R. G otter, A. Morgante, and F. Tommasini, Phys. Rev. Lett. 79 (1997) 1527.
- [6] M. Jalochocki, E. Bauer, H. Knoppe, and G. Lilienkamp, Phys. Rev. B 45 (1992) 13607.
- [7] R. J. Hamers, R. M. Tromp, and E. J. Fenuh, Phys. Rev. Lett. 56 (1986) 1972.
- [8] I. B. Altshuler, D. M. Chen, and K. A. M atveev, Phys. Rev. Lett. 80 (1998) 4895.
- [9] O. Gurlu, H. J. Zandvliet, and B. Poelsen a, Phys. Rev. Lett. 93 (2004) 066101.
- [10] W. B. Su, S. H. Chang, W. B. Jian, C. S. Chang, L. J. Chen, and T. T. T song, Phys. Rev. Lett. 86 (2001) 5116.
- [11] M. Jalochocki, Progr. Surf. Sci. 74 (2003) 97.
- [12] J. Terso, D. R. Hamann, Phys. Rev. Lett, 50 (1983) 1998.
- [13] H. Haug, A. P. Yauho, Quantum Kinetics in Transport and Optics of Semiconductors, Springer, Berlin (1996).
- [14] Y. Caley, H. Cohen, G. Cuniberti, A. Nitzan, D. Porath, Israel J. Chem. 44 (2004) 133.
- [15] M. Krawiec, T. Kwapinski, M. Jalochocki, phys. stat. sol. (b) 242 (2005) 332.
- [16] S. Hasegawa, X. Tong, S. Takeda, N. Sato, T. Nagao, Progr. Surf. Sci. 60 (1999) 89.